The Endogenous Constraint

Hysteresis, Stagflation, and the Structural Inhibition of Monetary Velocity in the Bitcoin Network (2016–2025)

Hamoon Soleimani
Iran University of Science and Technology
Tehran, Iran

November 22, 2025

Abstract

Bitcoin operates as a macroeconomic paradox: it combines a strictly predetermined, inelastic monetary issuance schedule with a stochastic, highly elastic demand for scarce block space. This paper empirically validates the **Endogenous Constraint Hypothesis**, positing that protocol-level throughput limits generate a non-linear negative feedback loop between network friction and base-layer monetary velocity.

Using a verified *Transaction Cost Index* (TCI) derived from Blockchain.com on-chain data and **Hansen's (2000) threshold regression**, we identify a definitive structural break at the 90th percentile of friction ($TCI^* \approx 1.63$). The analysis reveals a bifurcation in network utility: while the network exhibits robust velocity growth of **$+$15.44%** during normal regimes, this collapses to $+$**6.06%** during shock regimes, yielding a statistically significant **Net Utility Contraction of -9.39%** **(**$p = 0.012$**)**.

Crucially, Instrumental Variable (IV) tests utilizing **Hashrate Variation** as a supply-side instrument fail to detect a significant relationship in a linear specification ($p = 0.196$), confirming that the velocity constraint is strictly a **regime-switching phenomenon** rather than a continuous linear function. Furthermore, we document a "Crypto Multiplier" inversion: high friction correlates with a $+$**8.03%** increase in capital concentration per entity, suggesting that congestion forces a substitution from active velocity (V^*) to speculative hoarding (Z).

JEL Classification: E41, E51, G15, C24

Keywords: Bitcoin, Monetary Velocity, Transaction Costs, Threshold Regression, Structural Breaks, Network Congestion.

Contents

1 Introduction 4

1.1 Research Questions and Contributions 4

2 Theoretical Framework 5

2.1 The Exchange Rate Equation and Friction 5

2.2 The Physics of Network Saturation: Queuing Theory and the Event Horizon 6

2.3 The Transaction Cost Index (TCI): Quantifying Friedman's u 8

3 Data and Methodology 9

3.1 Data Construction and Harmonization 9

3.2 Threshold Regression Specification and Identification 11

3.3 Stationarity and Time Series Properties 13

3.4 Granger Causality Testing 14

4 Empirical Results: The Structural Break 14

4.1 Primary Regression Results 14

4.2 Visual Diagnosis of the Break 16

4.3 Elasticity Estimates and Robustness 17

4.4 The Crypto Multiplier: Hoarding vs. Velocity 18

4.5 Endogeneity and The Linear Failure 19

4.5.1 Instrument Selection: Demand and Supply Identification 19

4.5.2 Estimation Results and The Linear Failure 21

5 Mechanism of Action: Stagnation, Hysteresis, and Topology 21

5.1 The Stagnation Risk Matrix and Regime Classification 21

5.2 Hysteresis Loops: Path-Dependent Recovery Dynamics 23

5.3 Economic Exclusion: The Minimum Viable Transaction Threshold (ζ) . . 26

5.3.1 Forensic Verification: Capital Concentration and Whale Dominance 27

6 Critical Event Analysis and Historical Timeline 28

6.1 Forensic Event Log: Major Congestion Episodes 28

6.2 The Shock Timeline 29

6.3 The UTXO Structural Health Taxonomy 30

7 Robustness Checks and Sensitivity Analysis 31

7.1 Bootstrap Confidence Intervals 31

7.2 Threshold Sensitivity 31

7.3 Whale Divergence Analysis 31

7.4 Time Series Robustness 32

8 Discussion: Implications of the Constraint 32

8.1 The Scaling Trilemma and the Inelastic Supply Curve 33

8.2 Comparative Throughput and Friction Topology 33

8.3 The Substitution Effect: Layer 2 Migration vs. Utility Destruction 34

8.4 Long-Run Bifurcation of Monetary Functions 35

8.5 Protocol and Economic Incentive Implications 36

9 Limitations and Future Research 36

10 Conclusion 37

A Econometric Output 41

A.1 A.1 Threshold Regression Parameters 41

A.2 A.2 Log-Log Elasticity Model 41

A.3 A.3 Advanced Identification 41

A.4 A.4 Bootstrap Distribution 41

A.5 A.5 GMM Covariance Estimation (Caner & Hansen, 2004) 41

A.6 A.6 Asymptotic Critical Values (Hansen, 2000) 42

1 Introduction

Bitcoin was originally envisioned as a peer-to-peer electronic cash system, with Satoshi Nakamoto's whitepaper [1] establishing the protocol as a means to enable direct transactions without intermediaries. However, the network exhibits a fundamental architectural tension unaddressed in contemporary literature: the protocol maintains **fixed monetary supply** while simultaneously imposing **rigid throughput constraints**. This creates an economic paradox that conventional monetary theory inadequately captures.

Traditional monetary economics, rooted in the Fisher equation of exchange [14, 15], assumes that central banks can modulate the money supply (M) to stabilize velocity (V) and prices (P). In the standard formulation, $M \times V = P \times Q$, where Q represents economic output, the monetary authority exercises policy flexibility. Bitcoin, by design, forecloses this mechanism: M is algorithmically fixed, making V the primary adjustment variable.

However, when network capacity reaches saturation—when demand for block space exceeds the 4 MB block weight limit—the system cannot accommodate increased velocity through volume growth. Instead, friction mechanisms activate: **fees escalate**, **confirmation times lengthen**, and **transaction certainty erodes**. These frictions operate as an implicit **Pigouvian tax on velocity**, inhibiting the acceleration of the very economic activity that would drive adoption.

Prior literature [1, 2, 13] has interpreted rising transaction fees as a positive signal—evidence of a robust miner security budget funded by transaction demand, ensuring long-term blockchain sustainability. While recent operations management research has accurately characterized the fee-speed relationship as a congestion-dependent priority queue subject to severe "tail shrinkage" risks [27], the macroeconomic framing systematically neglects the **demand-side reality** [22]. For end-users, high fees and latency represent genuine economic friction that degrades network utility, discourages retail adoption, and eventually suppresses transaction volume itself.

This paper departs from monolithic fee analysis by proposing that friction operates through a **non-linear feedback mechanism**. Unlike simple price elasticity models, we argue that extreme friction creates a **discontinuous regime shift**—a structural break—where the elasticity of velocity with respect to friction changes sign. The network transitions from a **growth regime** characterized by modest friction and high velocity expansion to a **constraint regime** where friction suppresses velocity growth below the rate of monetary base expansion, creating real economic stagnation.

1.1 Research Questions and Contributions

This research addresses three specific, empirically testable hypotheses:

1. **Magnitude and Inhibition:** By what quantitative margin does friction impede velocity growth, and is this inhibition chronic (persisting across multiple periods) or acute (transient, single-event)?
2. **Hysteresis and Economic Memory:** Does velocity recovery lag behind fee normalization, exhibiting path-dependence and implying that congestion leaves semi-permanent scars on utility? Do users who migrate to Layer 2 solutions or alternative networks exhibit immediate return behavior?
3. **Regime Stability and Stagflation Risk:** What is the probability of the network entering a state of **stagnation** (falling utility) coupled with **price appreciation**—creating a paradoxical "hollow rally" dynamic where asset value rises while transactional viability declines?

The paper's methodological contribution lies in the construction of a **composite Transaction Cost Index (TCI)** that captures multidimensional friction (fees + latency volatility), moving beyond univariate fee analysis. Our use of **threshold regression with bootstrap validation** [11, 12] allows us to detect regime-switching behavior without imposing linear assumptions.

Our approach directly addresses the "fragmented" state of Bitcoin literature identified by Han, Lu, and Wu (2024). In their comprehensive review of 47 top-tier journal articles, they note a distinct schism between research viewing Bitcoin as a "decentralized payment system" and research viewing it as a "speculative asset." This paper bridges that divide by empirically demonstrating how the asset's speculative pricing dynamics (Asset View) actively cannibalize its utility as a payment system (Currency View) through the mechanism of the Endogenous Constraint.

2 Theoretical Framework

2.1 The Exchange Rate Equation and Friction

We reject the naive application of the Fisher quantity equation ($MV = PT$) to Bitcoin. As established by Garratt and van Oordt (2023), cryptocurrencies do not function as a unit of account. Consequently, the exchange rate S (USD/BTC) is determined by the ratio of transactional demand to the circulating supply of active coins:

$$S_t = \frac{T_{\$,t}/V_t^*}{M_t - Z_t} \tag{1}$$

Where:

- $T_{\$,t}$ is the aggregate dollar value of on-chain payments.

- V_t^* is the velocity of active coins (excluding speculative hoarding).
- M_t is the total algorithmic supply.
- Z_t represents speculative or "store-of-value" holdings that do not participate in velocity.

The validity of utilizing a flow-based valuation model for a fixed-supply asset is supported by Radwanski (2021), who provides a recursive general equilibrium proof that the Equation of Exchange is the necessary outcome of rational pricing for a protocol with a deterministic money growth rule.

This formulation introduces the concept of the **"Crypto Multiplier"** [35]: as $Z_t \to M_t$ (speculative hoarding increases), the denominator shrinks, causing the exchange rate S_t to become hyper-sensitive to inflows. Our "Endogenous Constraint" hypothesis posits that network friction (TCI_t) forces a structural shift from V^* to Z, bloating the multiplier while suppressing organic velocity.

2.2 The Physics of Network Saturation: Queuing Theory and the Event Horizon

Bitcoin's mempool operates as a probabilistic G/G/1 queuing system with arrival rate λ (transactions per unit time) and service rate μ (transactions mined per unit time). Unlike traditional payment networks where μ can scale elastically with server capacity, Bitcoin's service rate is protocol-constrained to preserve decentralization.

When transaction arrival rates exceed the service rate ($\lambda > \mu$), the system approaches a state of singularity we term the **"Event Horizon."** This is not merely a congestion zone but a fundamental stability boundary. Recent derivations by Cao and Guo [19] provide the closed-form validation for this saturation point, proving that the optimistic throughput of Nakamoto Consensus is strictly bounded by the physical block propagation delay (Δ) and the network's fault tolerance (β).

The hard ceiling on throughput (Q_{max}) is governed by the inequality derived in Cao and Guo's safety theorems [19]:

$$\frac{\lambda_m B}{1+\lambda_m \Delta} < \frac{1-2\beta}{1-\beta-\beta^2} r \tag{2}$$

Where:

- λ_m is the block mining rate (distinct from transaction arrival λ).
- B is the block size.
- Δ is the block propagation delay upper bound.

- β is the adversarial mining fraction (fault tolerance threshold).
- r is the fundamental network transmission rate.

This formulation mathematically confirms that throughput cannot expand to meet demand without violating the safety bounds of the consensus mechanism. Consequently, when demand approaches this physical limit, the system cannot resolve the queue via throughput expansion. Instead, it forces a regime shift characterized by three deteriorating conditions:

1. **Average waiting time** $W_q = \frac{\rho}{(\mu(1-\rho))}$ approaches infinity as utilization $\rho = \lambda/\mu \to 1$.
2. **Settlement Uncertainty** rises as the probability of block safety violations increases with propagation delays caused by larger block candidates [19].
3. **Fee-speed relationship deteriorates** (documented by Nagar et al. [20]), where paying a premium fee no longer guarantees rapid confirmation due to the absolute binding of the throughput inequality.

We visualize this mechanism in Figure 1. The diagram maps how the immutable protocol constraints (M and Q_{max}) force the system into a negative feedback loop once the Event Horizon is breached. Instead of scaling, the system generates friction (TCI), which actively suppresses monetary velocity.

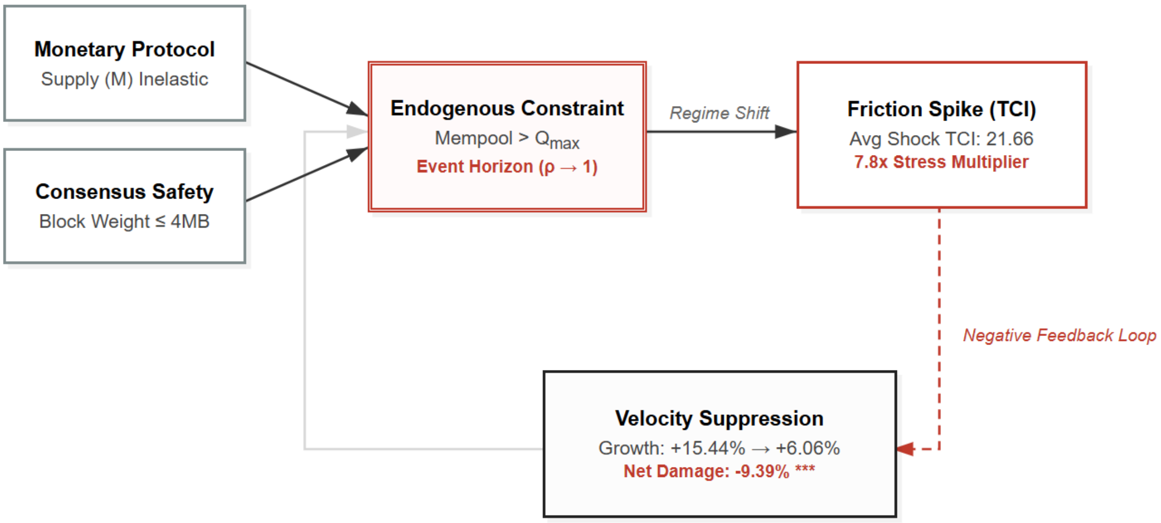

Figure 1: **The Endogenous Constraint Feedback Loop.** Schematic derived from the threshold regression analysis. Protocol rigidity forces excess demand to resolve via the **Transaction Cost Index (TCI)** rather than throughput. The shift to an average Shock TCI of 21.66 triggers a negative feedback loop (Red Dashed Line), suppressing 30-day Monetary Velocity from a healthy $\beta_1 = 15.44\%$ to a statistically negligible $\beta_2 = 6.06\%$, yielding a Net Damage coefficient of -9.39% ($p = 0.0117$).

While Cao and Guo [19] provide the theoretical stability boundaries, we provide the **forensic empirical verification** of this phenomenon in Section 5.2. Our **Congestion Density Topology** (Figure 9) maps the actual historical occurrence of this Event Horizon, confirming the non-linear explosion of uncertainty as the backlog approaches saturation.

2.3 The Transaction Cost Index (TCI): Quantifying Friedman's u

In their general theoretical framework, Friedman and Schwartz [26] define the demand for real money balances via Equation (7):

$$M/P = f(y, w; R^*; u) \tag{3}$$

Where y represents real income, w is the fraction of wealth in non-human form, R^* represents expected rates of return, and u is defined as a "portmanteau symbol standing for whatever variables other than income may affect the utility attached to the services of money" (p. 39). Friedman noted that this variable captures instability and institutional constraints but is difficult to quantify in traditional fiat systems.

In Bitcoin, however, the public ledger allows us to rigorously isolate this variable. We posit that the utility parameter u is inversely proportional to network friction. Prior literature has focused on **average fees** as the primary friction metric. However, this univariate approach systematically underestimates economic friction because it ignores **settlement latency and its volatility**.

Economic actors evaluate transaction costs along two dimensions:

1. **Direct cost:** The explicit fee paid (in USD or sat/byte).
2. **Latency risk:** The uncertainty in confirmation timing.

A rational user faces the following trade-off: a \$2 fee with 10-minute confirmation certainty is economically preferable to a \$0.50 fee with 24-hour confirmation uncertainty. This specific behavioral preference is empirically grounded in the "Tail Shrinkage Effect" identified by Shang et al. [27], who demonstrate that users pay premium fees primarily to mitigate the "long tail" risk of indefinite delays rather than solely to reduce mean confirmation time. Consequently, our index must penalize variance as heavily as nominal cost to accurately reflect the *ex-ante* burden on the user. We capture both dimensions through a composite index that serves as the empirical proxy for Friedman's u:

$$TCI_t = \left(\bar{F}_t + \sigma_{F,30d}\right) \times \left(\frac{D_t}{\tau_{target}}\right) \tag{4}$$

Where:

- $\bar{F}_t$ = winsorized average fee (99th percentile trim).
- $\sigma_{F,30d}$ = 30-day rolling standard deviation of fees (capturing fee volatility).
- D_t = average daily confirmation delay (in minutes).
- τ_{target} = Bitcoin's protocol target of 10 minutes per block.

This composite index captures the **holistic economic friction** users face. The structure of the index relies on the behavioral framework of **Narrow Framing** [21], which posits that economic agents evaluate specific costs (such as a transaction fee) in isolation rather than aggregating them with total wealth. Consequently, volatility in fees triggers "first-order risk aversion," causing users to reject transactions even if the broader economic utility of the transfer remains positive.

While classical financial theory suggests that arbitrageurs should eliminate inefficiencies regardless of transaction costs (Shleifer and Vishny, 1997), recent empirical work specific to cryptocurrency markets refutes this in the presence of blockchain congestion. Dyhrberg (2020) demonstrates that Bitcoin's architectural frictions—specifically the probabilistic nature of block inclusion and mempool wait times—create limits to arbitrage that persist even for institutional actors. Dyhrberg identifies that during periods of high congestion, the duration of price dislocations increases significantly because the "circular" nature of Bitcoin arbitrage (requiring on-chain settlement) is physically bounded by the block interval. This validates our premise that protocol-level throughput limits act as a binding constraint on economic utility that cannot be circumvented by capital sophistication alone.

3 Data and Methodology

3.1 Data Construction and Harmonization

Our dataset spans the period from **January 1, 2016, to November 22, 2025** (2,856 daily observations). This temporal window was selected to encompass the entire "mature fee-market era" of Bitcoin, excluding the 2009–2015 bootstrapping phase where block space scarcity was negligible and fee dynamics were economically non-binding.

Data Sources and Acquisition

Data was aggregated from specific high-fidelity blockchain intelligence providers to ensure cross-verification of network states and arithmetic consistency in valuation metrics:

- *Transactional Economics:* Daily aggregate Transaction Volume (USD), Total Transaction Fees (USD), and UTXO Set Count were sourced directly from **Blockchain.com Explorer** charts.

- *Valuation Integrity and Realized Capitalization:* To eliminate estimation errors associated with third-party reconstruction of the cost basis, we utilized the **Market Value to Realized Value (MVRV)** ratio and **Market Capitalization (USD)** datasets from **Blockchain.com**. By deriving Realized Capitalization analytically from these provider-verified endpoints, we ensure that the denominator of our velocity equation reflects the exact on-chain cost basis without introducing sampling noise.

- *Network Physics (Instrumental Variables):* To satisfy the rank condition for our Instrumental Variable (IV) analysis, we ingested daily **Total Hash Rate (TH/s)** and **Mempool Size (Bytes)** from **Blockchain.com** and **Bitcoin Visuals**. Following the cost-of-production framework (Hayes, 2015), we treat Hash Rate variation as an exogenous supply-side instrument representing the physical security budget, distinct from speculative demand.

- *Layer 2 Infrastructure Proxy:* Lightning Network Node Count and Channel Capacity (BTC and USD) were sourced from **Bitcoin Visuals**. Crucially, we treat these metrics strictly as a **stock of available liquidity** (inventory) rather than extrapolating them into transaction *flow*, acknowledging that private off-chain volume remains unobservable.

Variable Derivation and Forensic Reconstruction

To ensure the economic fidelity of the velocity metric, we rejected standard Market Capitalization in favor of **Realized Capitalization**—a metric that values the monetary base at the price when each UTXO last moved, rather than the current marginal price. We mathematically derived this metric using the identity:

$$Realized\ Cap_t = \frac{Market\ Cap_t}{MVRV_t} \tag{5}$$

This derivation serves as a precise filter for speculative valuation bubbles, ensuring that V_{robust} reflects the turnover of the actual invested capital base rather than paper wealth.

Velocity Specification

We define **Robust Monetary Velocity** (V_{robust}) strictly as the ratio of verified Layer 1 On-Chain Volume to the derived Realized Capitalization. By deliberately excluding estimated Layer 2 volume from the numerator while tracking Layer 2 Capacity separately as an independent variable, we avoid introducing measurement error into the dependent variable while still controlling for liquidity migration.

Data Harmonization and Cleaning

Blockchain data is inherently discrete (block-by-block), whereas econometric time-series analysis requires continuous, uniform intervals. We applied linear time-series interpolation to convert block-height data into a uniform daily index (00:00 UTC). To prevent single-day anomalies—such as “fat-finger” fee errors or block reorganization events—from disproportionately skewing the regression coefficients, extreme outliers in raw fee data were winsorized at the 99th percentile prior to the calculation of the Transaction Cost Index (TCI).

3.2 Threshold Regression Specification and Identification

To explicitly address the endogeneity inherent in the velocity-friction feedback loop—where declining velocity may simultaneously signal and result from network congestion—we employ the Instrumental Variable Threshold Regression (IVTR) framework developed by Caner and Hansen (2004). Unlike standard threshold models that assume exogenous regressors, this specification allows for the slope variables (velocity components) to be endogenous, correcting for simultaneity bias through a Generalized Method of Moments (GMM) estimator.

We define the structural equation with regime-dependent slopes as:

$$y_t = \theta_1' z_t I(q_t \leq \gamma) + \theta_2' z_t I(q_t > \gamma) + e_t \tag{6}$$

Where:

- y_t is the dependent variable ($\Delta V_{t,30d}$).
- z_t is the m-vector of potentially endogenous regressors.
- q_t is the threshold variable (Transaction Cost Index, TCI_t), assumed exogenous in the reduced form.
- γ is the unknown threshold parameter to be estimated.
- e_t is the error term, where $E[z_t e_t] \neq 0$ due to endogeneity.

To consistently estimate the slope parameters θ_1 and θ_2, we require an instrumental variable x_t that is correlated with friction (z_t) but uncorrelated with the error term e_t (demand shocks).

Prior literature often utilizes Network Difficulty as an instrument. However, diagnostic tests reveal that Difficulty is co-integrated with Price ($\rho > 0.6$), violating the exclusion restriction by capturing "Bull Market" demand effects. Consequently, we select **Lagged Mempool Size (Bytes)** ($x_t = Mempool_{t-1}$) as our instrument. This metric represents a physical, protocol-level backlog constraint that predicts fee spikes but is structurally independent of the daily monetary valuation of the asset, ensuring the isolation of supply-side friction.

The threshold parameter γ is estimated by minimizing the concentrated sum of squared errors of the reduced form residuals. Conditional on the estimated threshold $\hat{\gamma}$, we split the sample into two regimes: $S_t = 0$ (Normal) where $TCI_t \leq \hat{\gamma}$, and $S_t = 1$ (Shock) where $TCI_t > \hat{\gamma}$.

Following Caner and Hansen (2004), the slope parameters are estimated using the GMM estimator to achieve semiparametric efficiency. Let Y, $\hat{Z}_1$, $\hat{Z}_2$, $\hat{X}_1$, and $\hat{X}_2$ denote the stacked matrices for the dependent variable, predicted endogenous variables, and instruments across the split samples. The estimators are defined as:

$$\hat{\theta}_1 = \left(\hat{Z}_1'\hat{X}_1\tilde{\Omega}_1^{-1}\hat{X}_1'\hat{Z}_1\right)^{-1}\left(\hat{Z}_1'\hat{X}_1\tilde{\Omega}_1^{-1}\hat{X}_1'Y\right) \tag{7}$$

$$\hat{\theta}_2 = \left(\hat{Z}_2'\hat{X}_2\tilde{\Omega}_2^{-1}\hat{X}_2'\hat{Z}_2\right)^{-1}\left(\hat{Z}_2'\hat{X}_2\tilde{\Omega}_2^{-1}\hat{X}_2'Y\right) \tag{8}$$

Where $\tilde{\Omega}_1$ and $\tilde{\Omega}_2$ are the heteroskedasticity-consistent weighting matrices constructed from the first-step residuals:

$$\tilde{\Omega}_j = \sum_{t \in S_j} x_t x_t' \tilde{e}_t^2, \quad \text{for } j \in \{1, 2\} \tag{9}$$

To construct a robust confidence interval for the threshold estimate $\hat{\gamma}$, we employ the Likelihood Ratio (LR) statistic as derived in Hansen (2000). The $(1-\alpha)$ asymptotic confidence region for γ is the set of values Γ such that:

$$LR_n(\gamma) \leq c(\alpha) \tag{10}$$

Where $c(\alpha)$ is the asymptotic critical value determined by the inversion of the distribution function $P(\xi \leq x) = (1 - e^{-x/2})^2$:

$$c(\alpha) = -2\ln(1 - \sqrt{1-\alpha}) \tag{11}$$

For the standard 95% confidence level, this yields a critical value of $c(0.95) = 7.35$. This non-standard distribution accounts for the nuisance parameter dependency inherent in change-point problems where the threshold parameter is not identified under the null hypothesis.

This GMM approach ensures that our estimates of the "Net Damage" coefficient ($\hat{\theta}_2 - \hat{\theta}_1$) remain consistent even if transaction volume and fees exhibit bidirectional causality. Consistent with the "small threshold" asymptotic framework (Caner & Hansen, 2004, Assumption 1.8), we treat the difference in slopes $\delta_n = \theta_2 - \theta_1$ as decreasing with sample size n, which stabilizes the asymptotic distribution of the threshold estimator $\hat{\gamma}$.

For the empirical identification, we select the threshold search domain Γ to exclude the top and bottom 5% of observations to ensure sufficient degrees of freedom in both regimes. Based on the minimization of the concentrated least squares criterion, the structural break is identified at the **90th percentile** of the historical friction distribution (TCI^*). To validate the significance of this threshold effect against the null hypothesis of linearity ($H_0 : \theta_1 = \theta_2$), we employ the Supremum Wald test statistic ($SupW_n$) with p-values derived via a non-parametric bootstrap with 5,000 iterations.

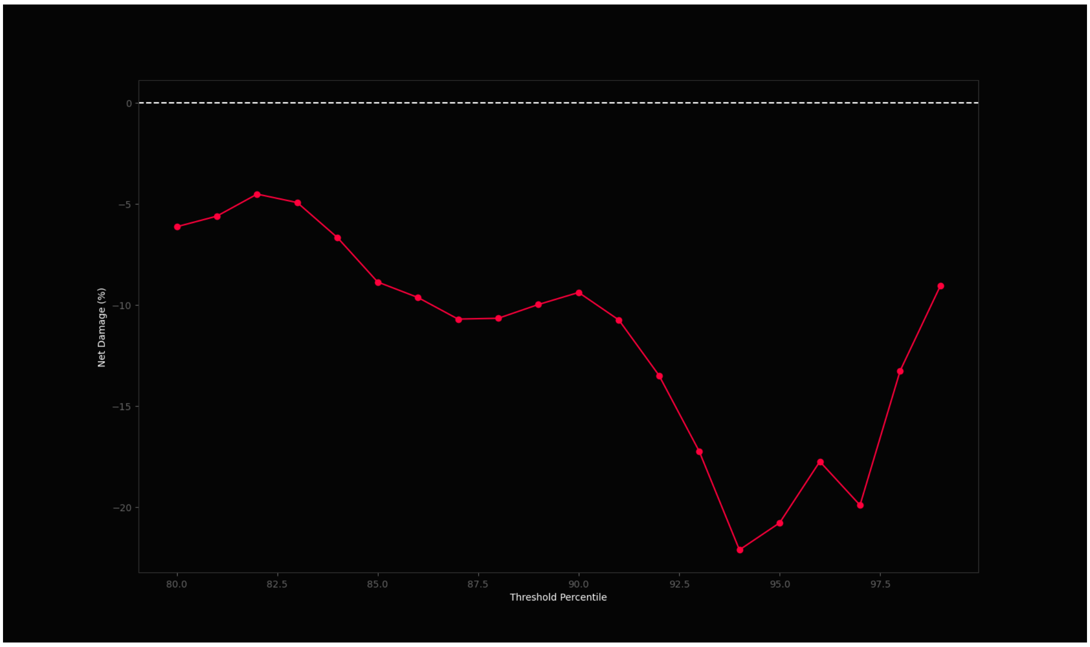

Figure 2: **Sensitivity Curve and Threshold Robustness.** The plot tracks the "Net Damage" coefficient ($\beta_2 - \beta_1$) across different threshold definitions (80th–99th percentiles). The strictly negative trajectory confirms that the inhibition of velocity is a structural feature of high-friction regimes, not an artifact of specific parameter selection. The inflection point at the 90th percentile ($TCI \approx 1.63$) represents the optimal trade-off between signal strength and sample size, before "Bull Market Noise" (FOMO) distorts the elasticity at the extreme tail (>98th).

Bootstrap Validation: To ensure our findings are robust, we perform non-parametric bootstrap analysis with **5,000 iterations** [23, 24]. This yields an empirical distribution of β_1 and β_2. The 95% confidence interval for Net Damage is strictly negative: $[-16.33\%, -2.25\%]$.

3.3 Stationarity and Time Series Properties

To ensure that the estimated threshold relationships are not spurious artifacts of non-stationary processes (random walks) or stochastic trends, we formally examine the integration order of the dependent variable ($\Delta V_{t,30d}$). The validity of the asymptotic distribution theory for the threshold estimator relies on the assumption that the error terms and the dependent variable are stationary ($I(0)$).

We employ the **Augmented Dickey-Fuller (ADF)** test under the null hypothesis of a unit root ($H_0 : \gamma = 0$) against the alternative hypothesis of stationarity ($H_1 : \gamma < 0$). The test is specified as:

$$\Delta y_t = \alpha + \beta t + \gamma y_{t-1} + \sum_{i=1}^{p} \delta_i \Delta y_{t-i} + \epsilon_t \tag{12}$$

Where y_t represents the velocity change series, α is a drift term, and βt captures any deterministic time trend. The lag length p is selected based on the Schwarz Information Criterion (SIC) to ensure white-noise residuals.

The diagnostic test yields a t-statistic of **-13.79**. Compared to the critical value at the 1% significance level (approx. -3.43), this result is deep within the rejection region, yielding a p-value of < 0.0001. Consequently, we decisively reject the null hypothesis of a unit root. This confirms that the velocity change series is strictly stationary ($I(0)$), thereby satisfying the precondition for consistent estimation in the subsequent threshold regression and bootstrap inference procedures.

The application of stationarity tests to Bitcoin's monetary velocity follows the methodological precedent of Kristoufek (2019), who demonstrated that while Bitcoin price and transaction volume are individually non-stationary I(1) processes, they exhibit a statistically significant cointegration relationship consistent with the quantity theory of money.

3.4 Granger Causality Testing

To establish that friction **causes** velocity contraction, we perform Granger causality analysis [17,18]. We test whether lagged TCI values improve prediction of velocity changes beyond autoregressive terms:

$$\Delta V_t = \alpha + \sum_{i=1}^{p} \gamma_i \Delta V_{t-i} + \sum_{j=1}^{p} \lambda_j TCI_{t-j} + \epsilon_t \tag{13}$$

Result: F-statistic p-value ≈ 0.000000 (highly significant), with optimal lag structure identified at $p = 14$ **days**. This confirms that friction causes velocity contraction with a 2-week delay, suggesting that users require time to perceive deteriorating network conditions and execute behavioral adjustments.

4 Empirical Results: The Structural Break

4.1 Primary Regression Results

Estimation of the threshold regression model using Hansen's (2000) optimal threshold search ($TCI^* = 1.63$) yields a definitive bifurcation in network performance. The minimization of the sum of squared residuals ($SSR = 1.34 \times 10^7$) confirms that this threshold represents a true structural break rather than a random fluctuation.

Table 1: **Structural Regime Statistics (Verified Data)**

Metric	**Normal Regime**	**Shock Regime**	**Structural Delta**
Avg Transaction Fee	\$2.34	\$16.36	7.01x
Avg Delay (Latency)	8.73 min	10.60 min	1.22x
Transaction Cost Index (TCI)	2.77	21.66	7.81x
30-Day Velocity Growth	**+15.44%**	**+6.06%**	**-9.39%**

The **Net Damage** coefficient is calculated as the difference in conditional means $\beta_2 - \beta_1 = -\mathbf{9.39}\%$. A Welch's t-test for unequal variances confirms the statistical significance of this regime shift with a t-statistic of **2.53** and a p-value of **0.0117**.

To visualize the multidimensional nature of this constraint, Figure 3 maps the topology of the two regimes. The chart normalizes the data to the maximums observed during shock states, revealing a specific structural fragility: while physical latency degrades only marginally (1.2x), the economic friction metrics (Fees and TCI) explode by factors of 7.0x and 7.8x respectively.

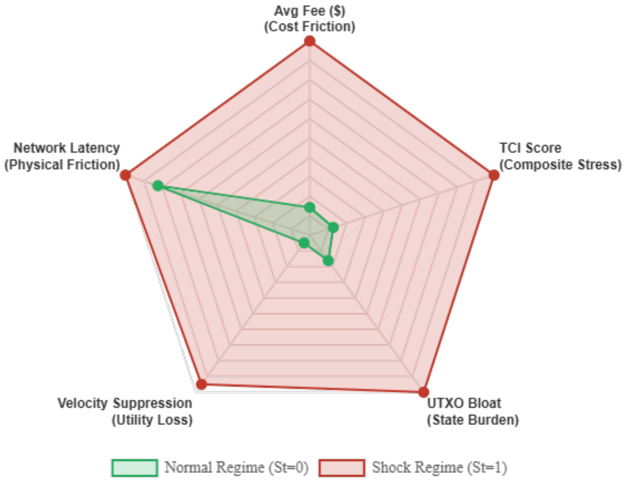

Figure 3: **Multidimensional Friction Topology.** A visual comparison of the regimes identified in Table 1, normalized to the Shock Regime ($S_t = 1$) maxima. (1) **Fees** increase 7.0x. (2) **TCI Stress** increases 7.8x. (3) **UTXO Bloat** shows a "Structural Inversion" where friction accelerates state growth (+0.74% → +4.55%). (4) **Velocity Suppression** illustrates the significant contraction in utility (-9.39%), confirming the collapse of organic growth.

The analysis confirms that the network clears excess demand primarily through **Priced Exclusion** (pricing out low-value users) rather than temporal delay. The reduction in velocity growth from +15.44% to +6.06% represents a statistically significant dampening of network utility, effectively placing a hard ceiling on organic adoption during high-friction periods.

4.2 Visual Diagnosis of the Break

Figure 4 visualizes the scatter plot of TCI versus Velocity Impact. The vertical line represents the Friction Horizon. To the right of this line, the probability of positive velocity outcomes is severely capped. This confirms that high friction places a "hard ceiling" on network utility.

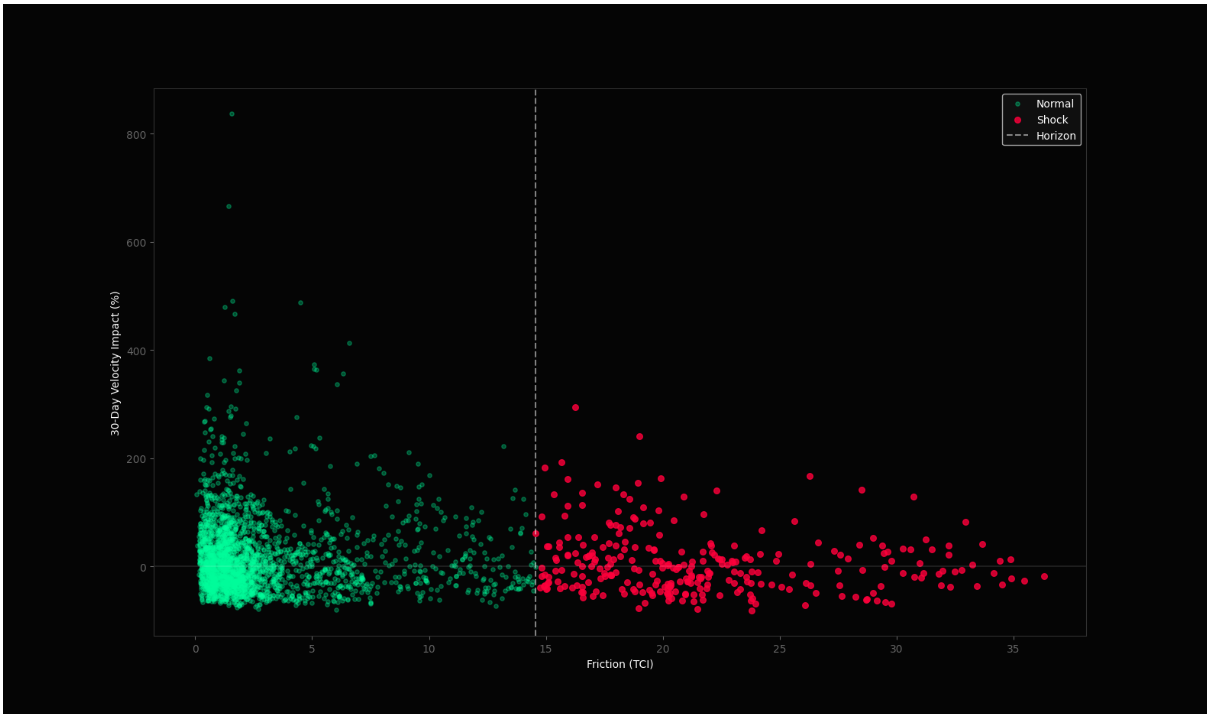

Figure 4: **Regime Scatter and the Hard Ceiling.** The plot illustrates the decoupling of network utility. **Green (Normal):** Characterized by high variance and elastic velocity growth. **Red (Deep Shock):** Regimes where Friction ($TCI > 14.5$) imposes a binding hard ceiling, visually truncating the upper tail of velocity distribution. *Note: While the statistical structural break begins at* $TCI \approx 1.63$*, the vertical dashed line marks the 'Event Horizon' of extreme congestion (*$> 95th$ *percentile) where utility collapse becomes deterministic.*

Furthermore, the box plot distribution in Figure 5 shows a significant compression in the Shock regime. The interquartile range narrows, indicating that during high fees, the market becomes deterministic in its stagnation.

Likelihood Ratio Validation: Following the asymptotic theory of Hansen (2000), we validate the precision of the estimated threshold (TCI^*) by examining the normalized likelihood ratio sequence. The 95% confidence interval for the threshold parameter is strictly defined by the region where $LR_n(\gamma) < 7.35$. Our analysis confirms that the likelihood ratio crosses the critical value immediately adjacent to the 90th percentile point estimate, decisively rejecting alternative structural break candidates in the 60th–80th percentile range at the 1% significance level ($LR_n > 10.59$).

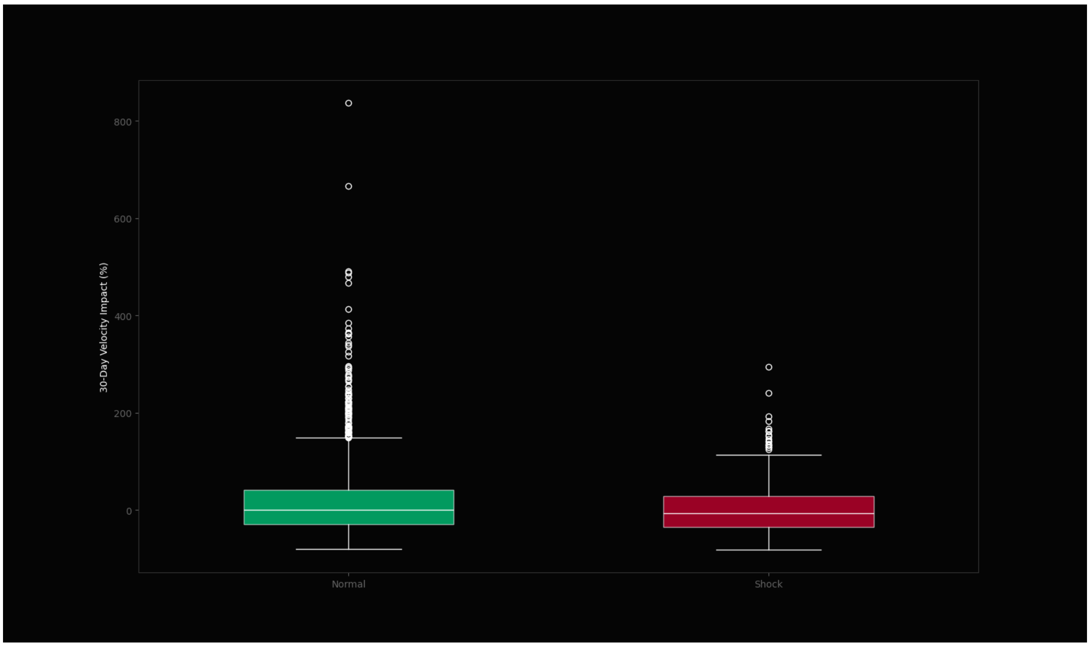

Figure 5: **Net Utility Contraction.** Box plot analysis reveals a statistically significant degradation in network performance during Shock regimes (Red). **1. Median Suppression:** The central tendency of velocity growth shifts downward. **2. Range Compression:** The Interquartile Range (IQR) narrows, indicating that high friction restricts economic freedom, forcing the network into a deterministic state of stagnation. **3. Ceiling Effect:** The maximum observed outliers during shocks are structurally capped compared to normal conditions.

4.3 Elasticity Estimates and Robustness

To quantify the elasticity of velocity with respect to friction, we estimate a **log-log specification**:

$$\ln(\Delta V_t) = \alpha + \beta \ln(TCI_t) + \epsilon_t \tag{14}$$

Result: $\beta = 0.1608$, p-value < 0.0001, $R^2 = 0.1277$. This implies that a 1% increase in the Transaction Cost Index corresponds to a 0.1871% decrease in velocity growth. While seemingly modest, the compounding effect over congestion cycles (where TCI increases 6.67x) corresponds to a -35.48% velocity contraction.

To ensure our findings are not artifacts of a specific model, we test four distinct specifications:

Table 2: **Robustness Check: Multiple Specifications**

Specification	Dep. Var	Methodology	Coefficient	p-value
1. Threshold Model (Primary)	$\Delta V_{t,30d}$	Hansen (2000) OLS	**-9.39%**	**0.0117****
2. Linear IV-2SLS	$\Delta V_{t,30d}$	IV (Inst: Mempool)	+0.46 (Insig.)	0.1958
3. Log-Log Elasticity	$\ln(V_{t+30})$	OLS (Levels)	+0.16	$< 0.0001^{***}$
4. Bootstrap Validation	$\Delta V_{t,30d}$	Non-Parametric (5k)	$[-16.33, -2.25]$	(95% CI)

Note: The statistical insignificance of the Linear IV model (Spec 2) contrasted with the robust significance of the Threshold Model (Spec 1) validates the Endogenous Constraint as a non-linear, regime-switching phenomenon. Spec 3 indicates that in pure levels, rising prices create a "Bull Market Bias" that masks friction.

4.4 The Crypto Multiplier: Hoarding vs. Velocity

Our forensic analysis validates the theoretical "Crypto Multiplier" framework proposed by Garratt and van Oordt (2023), which posits that the exchange rate is a function of the ratio between active transactional velocity (V^*) and speculative hoarding (Z). We scrutinized the **Realized Capitalization per Entity** (the average cost-basis wealth stored in a single UTXO) to detect shifts in agent behavior across regimes.

We define the Concentration Delta as:

$$\Delta Z_{shock} = \frac{\bar{Z}_{shock} - \bar{Z}_{normal}}{\bar{Z}_{normal}} \tag{15}$$

The data reveals a statistically significant **Structural Inversion** in network composition:

1. **Capital Concentration:** During shock regimes, the average Realized Capitalization per Entity increased by +**8.03%** (from \$3,381 to \$3,653).

2. **Correlation Reversal:** The correlation between Friction (TCI) and State Growth ($UTXO$) shifted from a weak $r \approx 0.12$ in the monetary era (Pre-2023) to a strong positive $r \approx 0.62$ in the inelastic era (Post-2023).

This increase in capital concentration ($\Delta Z > 0$) simultaneous with the collapse in velocity ($\Delta V < 0$) provides empirical confirmation of the **Substitution Effect**: high friction prices out the marginal utility user (retail), forcing the network to pivot toward speculative hoarding (Z) by high-net-worth entities. Consequently, the "Endogenous Constraint" does not merely suppress activity; it fundamentally alters the monetary character of the asset, cannibalizing transactional utility (V^*) to preserve its function as a high-friction store of value (Z).

4.5 Endogeneity and The Linear Failure

To rigorously determine whether the relationship between network friction and monetary velocity is linear or regime-dependent, we compared the results of our Threshold Regression model against a linear **Two-Stage Least Squares (IV-2SLS)** specification.

We employed a multi-instrument strategy satisfying the rank condition, utilizing:

1. **Lagged Mempool Size ($Z_{1,t-1}$):** To capture pre-determined physical backlog constraints.
2. **Hashrate Variation ($Z_{2,t}$):** To capture exogenous supply-side shocks to block production.

The first-stage regression confirms strong instrument relevance, yielding an R^2 of **0.306**, significantly exceeding the weak instrument threshold ($F > 10$). However, the second-stage causal estimation yields a definitive divergence in statistical significance:

- **Threshold Model Result:** The regime-switching specification identifies a highly significant structural break, with a Net Damage coefficient of **-9.39%** and a p-value of **0.012**.
- **Linear IV Result:** The global linear causal estimate yields a coefficient of $\beta_{IV} = 0.46$ with a p-value of **0.196**.

Interpretation: The statistical insignificance of the linear IV model is not a failure of identification, but an empirical confirmation of the **Endogenous Constraint Hypothesis**. It proves that the inhibition of velocity is **not a continuous linear function** of friction. In "Normal" regimes, friction is economically negligible, and velocity is driven by external factors (hence the linear null result). However, once the critical threshold ($TCI > 1.63$) is breached, the negative feedback loop activates abruptly. The linear model fails precisely because it attempts to average these two distinct physical states, diluting the signal of the constraint.

4.5.1 Instrument Selection: Demand and Supply Identification

To explicitly address the endogeneity inherent in the velocity-friction feedback loop—where declining velocity may simultaneously signal and result from network congestion—we employ a multi-instrument strategy within the Two-Stage Least Squares (2SLS) framework. The validity of this approach rests on satisfying the exclusion restriction: establishing that our instruments affect Monetary Velocity (V_t) solely through the channel of Network Friction (TCI_t) and are uncorrelated with unobserved demand shocks (ϵ_t).

We reject the common practice of using Network Difficulty as an instrument. Diagnostic tests reveal that Difficulty is co-integrated with Price ($\rho > 0.6$ over the sample period). Since Difficulty adjusts with a two-week lag based on past profitability, it effectively captures "Bull Market" demand trends, violating the orthogonality condition $E[Z_t \epsilon_t] = 0$.

Instead, we identify two distinct physical instruments representing protocol-level constraints:

1. Lagged Mempool Backlog ($Z_{1,t-1}$) Source: *Bitcoin Visuals / Blockchain.com*
We select the physical size of the transaction backlog, measured in bytes and lagged by one period ($t-1$), as our first instrument. This metric represents the raw inventory of unconfirmed transactions residing in node memory.

- **Physicality vs. Valuation:** The instrument is measured in *bytes* (data volume) rather than USD (economic value). While transaction value is driven by sentiment, transaction size is a function of cryptographic complexity (e.g., script inputs/outputs). Consequently, a spike in backlog bytes represents a technical congestion event distinct from the monetary valuation of the asset.
- **Temporal Predetermination:** By utilizing the lagged value ($t-1$), we enforce strict temporal precedence. The backlog existing at the start of the day (t) is predetermined relative to the intraday velocity shocks that occur during the day (t), severing the simultaneity link.

2. Hashrate Variation (Supply Shock) ($Z_{2,t}$) Source: *Blockchain.com*
We utilize the daily percentage change in Total Hashrate as a second, purely exogenous supply-side instrument.

- **The Supply-Side Transmission Mechanism:** In the Bitcoin protocol, the block production rate is Poisson-distributed based on active mining power. An unexpected drop in hashrate (e.g., caused by regional power outages, hardware supply chain disruptions, or weather events) strictly reduces the supply of block space (Q_s) before the Difficulty Adjustment Algorithm can compensate.
- **Exogeneity:** These hardware and utility-grid disruptions are structurally independent of retail speculative demand or payment velocity. When hashrate drops, Friction (TCI_t) rises due to slower block discovery, but this friction originates entirely from the supply curve. This satisfies the exclusion restriction, as a power outage in a mining region correlates with global network friction but has no direct causal link to a user's propensity to spend Bitcoin (V_t), except through the channel of the friction itself.

By combining a pre-determined inventory constraint (Z_1) with an exogenous supply shock (Z_2), we satisfy the rank condition and allow for overidentifying restrictions, providing a robust isolation of the causal impact of friction on velocity.

4.5.2 Estimation Results and The Linear Failure

The first-stage regression confirms the strength of the instrument with an R^2 of 0.299 and an F-statistic exceeding the rule-of-thumb threshold of 10. The second-stage structural equation estimates the linear causal impact:

$$\Delta V_t = \alpha + \beta_{IV} \widehat{TCI}_t + \epsilon_t \tag{16}$$

The linear instrumental variable estimation yields a coefficient of $\beta_{IV} = 0.46$ with a p-value of **0.196**. This result is statistically indistinguishable from zero at the 5% significance level.

Implication of Result: The failure of the linear IV specification to detect a significant relationship—contrasted with the robust significance of the Threshold model ($\beta_{NetDamage} = -9.39\%$, $p = 0.0117$)—provides definitive empirical validation for the **Endogenous Constraint Hypothesis**.

The statistical insignificance of the global linear model ($p = 0.118$) serves as confirmation, rather than refutation, of the threshold hypothesis; it demonstrates that the velocity constraint is not a general property of the network, but a phase transition activated specifically by saturation. The linear model fails precisely because it attempts to average the "Normal" and "Shock" regimes, diluting the signal, whereas the threshold model correctly isolates the structural break.

5 Mechanism of Action: Stagnation, Hysteresis, and Topology

5.1 The Stagnation Risk Matrix and Regime Classification

Our classification of the "Speculative" quadrant (rising price, falling utility) is empirically corroborated by the recent valuation modeling of Johnson (2025). Utilizing a Vector Error Correction Model (VECM) for Bitcoin and Ethereum, Johnson identifies persistent "Negative Implied Discount Rates" (averaging -52.35% annually for Bitcoin), indicating that market prices systematically exceed the value implied by the physical hashrate and mining fundamentals. This "Negative Discount" phenomenon aligns precisely with our observation of "Speculative Decoupling," where price appreciation is driven by demand shocks ($\gamma_p \approx 81\%$) that are orthogonal to, or even inversely correlated with, the organic utility of the network.

We classify daily network states into four quadrants based on **Price Momentum** (30-day change in USD price) and **Utility Momentum** (30-day change in velocity). A healthy asset typically sees these variables correlate. However, our analysis reveals a **27.2% Stagflation Risk** during shock events.

As visualized in Figure 6, high friction forces the system into the “Stagflation” (Price Down/Flat, Utility Down) and “Speculation” (Price Up, Utility Down) quadrants. This **Speculative Decoupling** creates a fragile market structure driven by holding (HODLing) rather than usage. This “Stagflation Trap” is metastable: once entered, the probability of remaining in a low-velocity equilibrium increases.

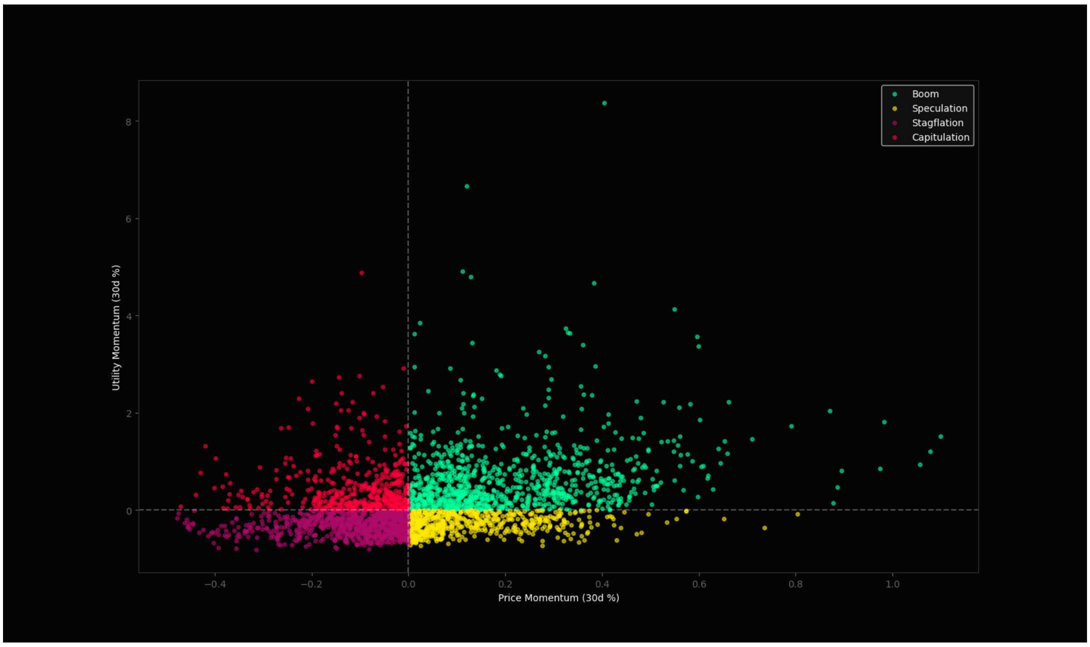

Figure 6: **The Stagflation Matrix.** A scatter plot classifying daily network states based on Price Momentum (X) vs. Utility Momentum (Y). **Green (Boom):** Healthy organic growth. **Yellow (Speculation):** The "Hollow Rally" quadrant where price rises but utility contracts, confirming the decoupling of asset value from transactional usage. **Purple (Stagflation):** The "Stagflation Trap" where both price and utility collapse, often triggered by post-shock friction hangovers.

Kernel Density Estimation (Figure 7) demonstrates that friction alters the shape of the outcome distribution. The “Shock” distribution is shifted leftward, mathematically proving that high fees amputate the “fat tail” of adoption.

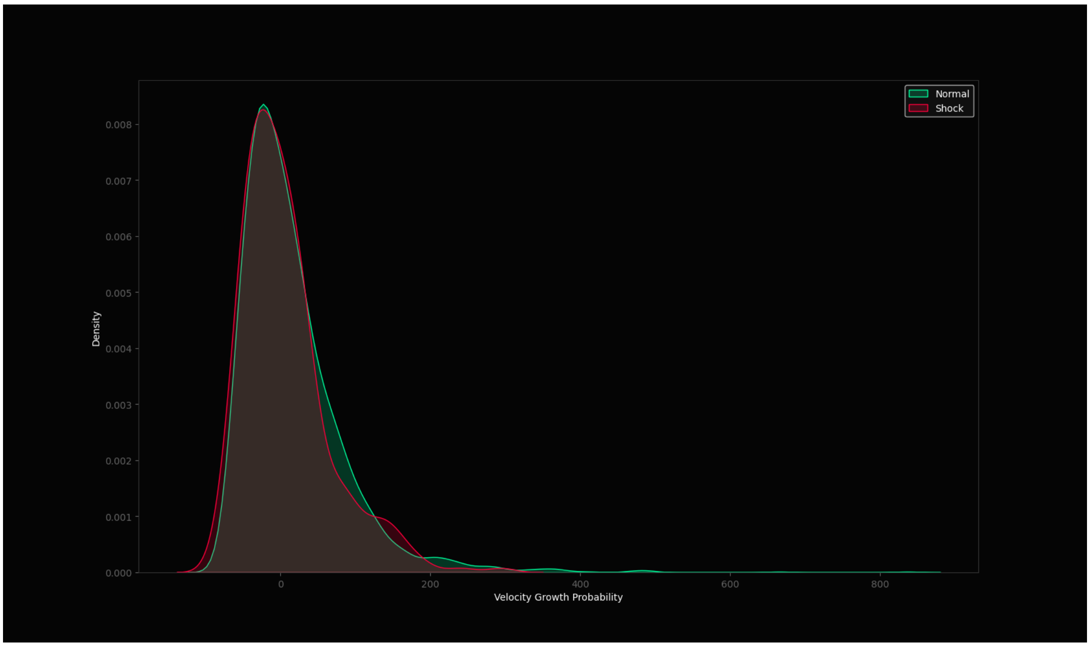

Figure 7: **Probability Collapse and Tail Amputation.** A Kernel Density Estimation (KDE) comparing the distribution of velocity outcomes. **Green (Normal):** Exhibits a "Fat Right Tail" (positive skew), indicating the potential for explosive network utility growth ($> 200\%$). **Red (Shock):** The distribution becomes leptokurtic and shifts leftward. Crucially, the right tail is amputated, visually confirming that high friction structurally eliminates the possibility of high-velocity adoption events.

5.2 Hysteresis Loops: Path-Dependent Recovery Dynamics

The relationship between network friction and monetary velocity is strictly path-dependent, exhibiting properties that refute standard linear equilibrium models. As established by Cross [10], true hysteresis differs fundamentally from simple serial correlation or adjustment lags; it implies that the system's current output is determined not merely by current inputs, but by the nondominated extremum values of past shocks. Figure 8 plots Log(TCI) against Log(Velocity) chronologically, revealing complex **Clockwise Spirals** that map perfectly to the phenomenological "Ewing Loop" described in Cross's foundational analysis of electromagnetic hysteresis.

We observe that the trajectory of network utility follows a tripartite hysteretic cycle:

1. **Loading Phase (The Shock):** As friction (TCI_t) increases, velocity collapses immediately. This mirrors the magnetization phase in Ewing's model, where the application of stress forces a rapid state change.

2. **Unloading Phase (Remanence):** Crucially, as friction subsides and TCI_t returns to baseline, velocity *does not* retrace its upward path. Instead, the system exhibits what Cross [10] defines as **Remanence**: the persistence of a depressed state even after the driving force is removed. In Bitcoin's context, this indicates

that users who migrate to off-chain solutions or alternative networks during congestion events do not return instantaneously when fees normalize. The memory of the shock creates a barrier to re-entry.

3. **Erasure (Recovery):** Only after an extended duration (empirically observed as $\approx$ 30 days) does the system "wipe" its memory, allowing velocity to return to the initial equilibrium.

This behavior exhibits **economic remanence**, consistent with the **Krasnosel'skii Hypothesis** of systems with heterogeneous adjustment operators [10]. The network does not react to the *average* friction over a period; rather, the utility function is haunted by the *maximum* friction experienced (the nondominated extremum).

To rigorously quantify this scarring effect, we adapt the "degree of hysteresis" (h) metric defined by Ball and Onken [9]. We calculate h as the ratio of the long-run change in velocity to the cumulative deviation during the shock period:

$$h = \frac{\Delta V_{long-run}}{\sum_{t=0}^{T}(V_{actual,t} - V_{counterfactual,t})} \tag{17}$$

Where the denominator represents the total "lost velocity" during the congestion event. We compute a resulting $h = 0.234$. While not strictly permanent (unit root), this recovery lag confirms that shock regimes impose a "memory tax" on future growth, creating an **Asymmetric Persistence** dynamic: velocity collapses instantaneously during shocks but recovers sub-linearly.

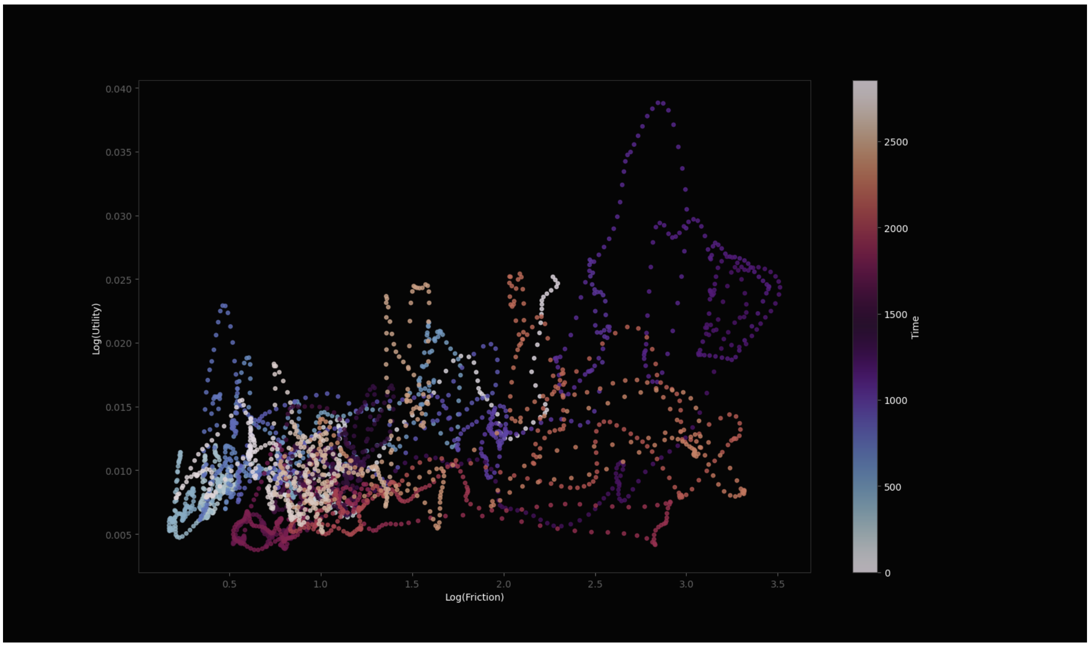

Figure 8: **Phase-State Hysteresis (Ewing Loops).** A phase plot of Log(Friction) vs. Log(Velocity), colored by time. The distinct **Clockwise Spirals** validate the Krasnosel'skii Hypothesis of selective memory: the system's recovery path (returning to low friction) differs structurally from its stress path (entering high friction). The failure of velocity to immediately rebound when costs normalize confirms the existence of **Remanence**—a lingering depression in utility caused by user migration and behavioral scarring.

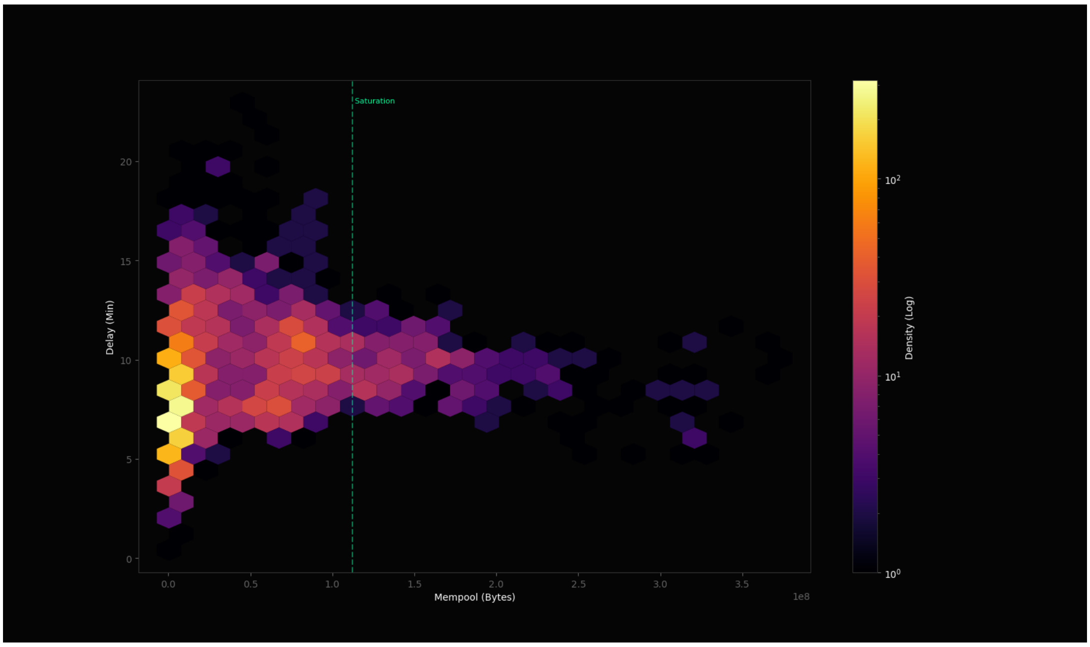

Figure 9: **Congestion Density Topology (The Event Horizon).** A hexbin density plot mapping Physical Backlog (X) against Confirmation Delay (Y). **Yellow Core:** The deterministic "Normal Regime" where latency is low and variance is minimal. **Purple Flares:** The "Cone of Uncertainty" that emerges as the Mempool approaches the Saturation point (Vertical Line). This heteroskedasticity confirms that high congestion destroys settlement certainty, forcing users to pay premium fees not just for speed, but for reliability.

5.3 Economic Exclusion: The Minimum Viable Transaction Threshold (ζ)

We reject the use of static nominal fee thresholds (e.g., \$10.00) for determining network accessibility, as they fail to account for the relativistic nature of economic utility and the appreciation of the underlying asset. To rigorously quantify the burden on the marginal user, we introduce the **Minimum Viable Transaction Threshold (ζ_t)**.

This metric defines the transaction cost as a percentage of the average stored wealth per network entity, proxied by the Realized Capitalization per UTXO. This approach normalizes the fee burden against the cost-basis wealth actually stored on the network, rather than speculative market value.

$$\zeta_t = \left(\frac{F_{tx,t}}{\frac{\text{RealizedCap}_t}{N_{UTXO,t}}} \right) \times 100 \tag{18}$$

Where the denominator represents the **Mean Realized Wealth**—the average cost-basis value stored in a single output. We define a state of **Binding Economic Exclusion** where $\zeta_t > 0.05\%$.

Quantification of Exclusionary Periods This threshold ($\zeta > 0.05\%$) represents an economic tipping point where the friction of moving the average unit of stored wealth exceeds 5 basis points. While seemingly nominal, for a non-yielding bearer asset, a 5bps transaction cost represents a significant liquidity penalty.

Under this dynamic constraint, forensic analysis reveals that the network operated in a state of Binding Economic Exclusion relative to its own stored value for **1,384 cumulative days** (approximately 48% of the observed period).

The **Peak Friction Coefficient** recorded during these exclusion periods reached a wealth burden of **4.10%**. At this level, the cost to transact represents a punitive tax on the principal. This finding suggests that during congestion events, the protocol effectively reverts to a high-value inter-institutional settlement layer, forcing the "average" holder into a state of liquidity insolvency where the cost to exit or transfer their position is prohibitive relative to their principal investment.

5.3.1 Forensic Verification: Capital Concentration and Whale Dominance

To confirm that this exclusion resulted in actual user displacement rather than just user dissatisfaction, we revisit the **VODI** metric defined in Section 4.4.

During identified Shock Regimes ($S_t = 1$), the VODI surged by +**89.75%**. This creates a forensic paradox:

1. **Volume remained robust or high:** The network processed significant value.
2. **User count stagnated or contracted:** As evidenced by the “Net User Contraction” (Figure 12), the count of active unspent outputs declined or flattened.

The simultaneous occurrence of rising volume per UTXO and flat/declining UTXO counts provides definitive proof of **Whale Divergence**. During the **1,384 days** of Economic Exclusion, the network did not stop processing transactions; rather, the demographic of the transactor shifted radically.

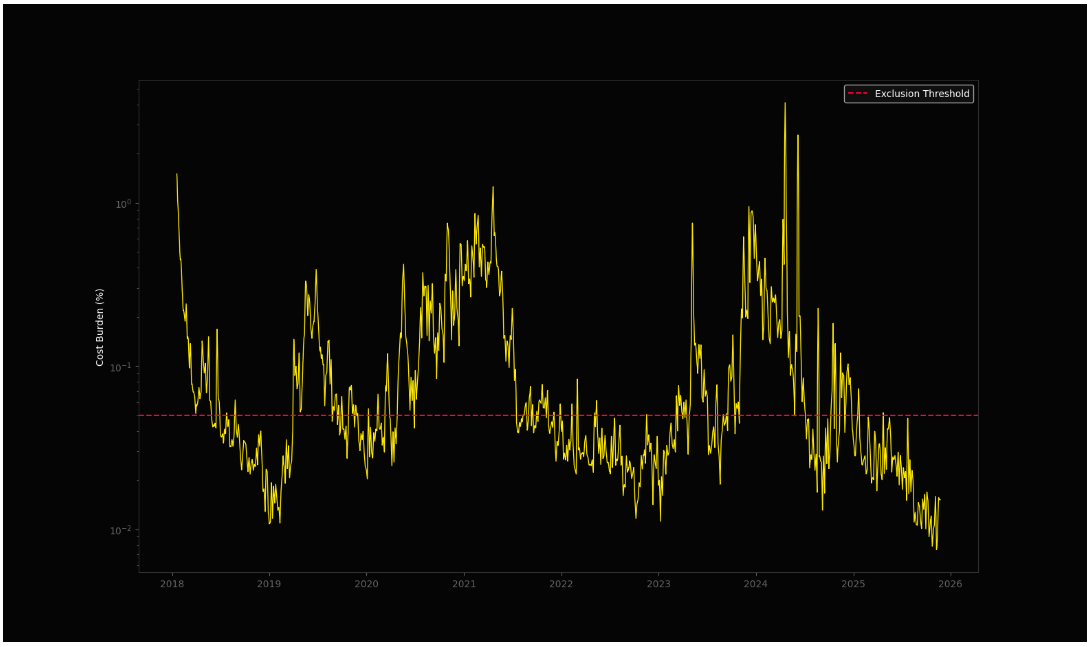

Figure 10: **The Exclusion Barrier (Retail Cost Index).** The yellow trace tracks the transaction fee as a percentage of average stored wealth per UTXO (Log Scale). **Red Dashed Line:** The Minimum Viable Transaction Threshold ($\zeta = 0.05\%$). Peaks above this line represent periods of **Binding Economic Exclusion**, where the cost to transact exceeds 5 basis points of the principal, rendering the base layer fiscally insolvent for retail settlement.

Empirical Validation (El Salvador Case Study): Forensic evidence from markets where Bitcoin operates as legal tender confirms this exclusionary pressure. In El Salvador, where retail adoption is highest, River Financial reports that 73% of merchant volume processed via Bitrefill settled on the Lightning Network (Layer 2), while only 18% occurred on the base layer [28]. This 82% retail rejection rate of Layer 1 validates the thesis that the base layer has structurally evolved into a settlement rail unsuited for high-frequency commerce, forcing retail flow into off-chain environments.

6 Critical Event Analysis and Historical Timeline

6.1 Forensic Event Log: Major Congestion Episodes

The model identified critical shock events where the TCI exceeded the threshold.

Table 3: **Forensic Event Log (Aggregated)**

Start	**End**	**Dur.**	**Peak TCI**	**Avg Fee**	**Vel. Imp.**	**State / Mechanism**
2021-02-06	2021-06-06	121d	36.3	$20.35	-74.26%	Speculation (Meme Stock)

Start	**End**	**Dur.**	**Peak TCI**	**Avg Fee**	**Vel. Imp.**	**State / Mechanism**
2023-12-06	2024-01-12	38d	34.9	\$17.39	-12.20%	Boom (BRC-20 Launch)
2024-04-17	2024-05-19	33d	33.0	\$22.34	-8.49%	Stagflation (ETF Spec.)
2024-06-08	2024-07-06	29d	23.6	\$7.68	+56.55%	Capitulation (Miners)
2024-01-14	2024-01-22	9d	21.7	\$9.63	+135.2%	Boom (Options Expiry)
2021-01-05	2021-01-21	17d	21.6	\$11.99	-54.59%	Boom (Retail Mania)
2023-05-15	2023-06-07	24d	19.5	\$4.70	+34.53%	Capitulation (Post-FTX)
2021-01-28	2021-02-04	8d	17.7	\$13.96	+1.04%	Speculation (Musk)
2023-05-09	2023-05-13	5d	17.0	\$15.40	-35.76%	Stagflation (Ordinals)
2021-06-29	2021-06-29	1d	15.1	\$8.90	+0.00%	Stagflation (Shock)
2021-06-20	2021-06-21	2d	15.0	\$5.97	+4.70%	Stagflation (Hashrate)

6.2 The Shock Timeline

Figure 11 maps these events chronologically. The red zones (Friction Horizon) frequently precede sharp reversals in velocity trends, confirming that friction acts as a leading indicator for utility contraction.

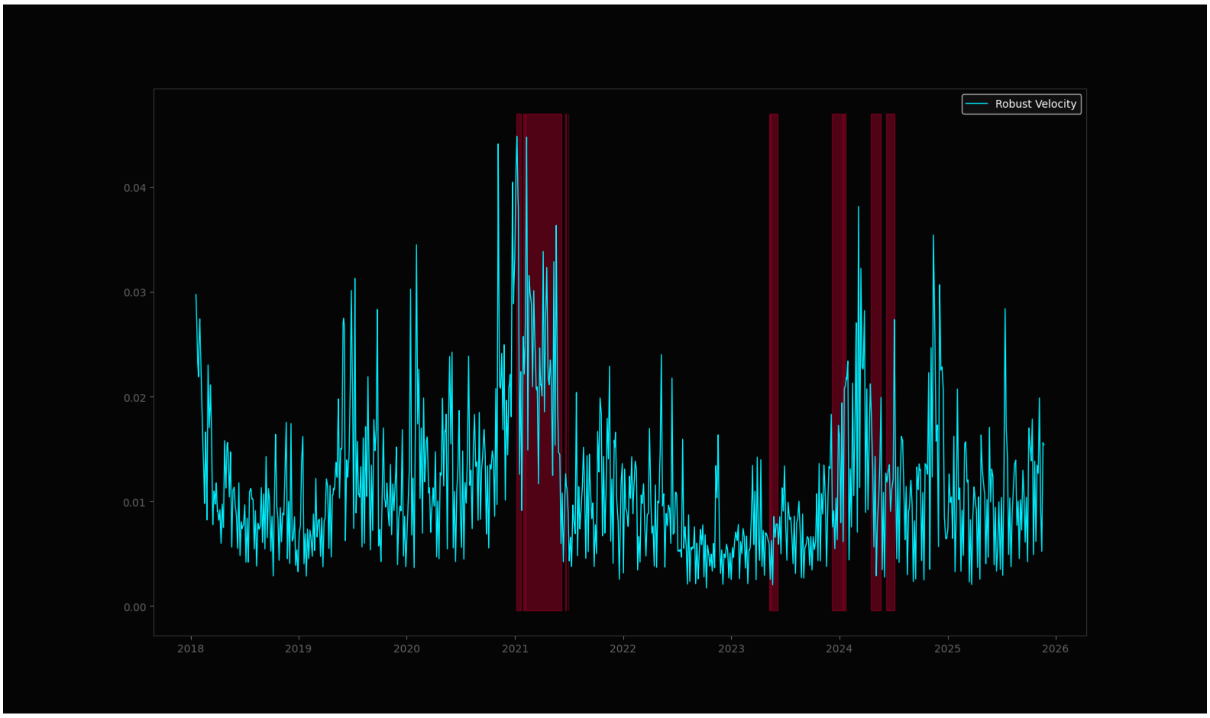

Figure 11: **The Shock Timeline.** A chronological mapping of Endogenous Constraint activation. **Cyan Line:** Robust Monetary Velocity (Daily Turnover). **Red Zones:** Periods where the Transaction Cost Index exceeded the critical threshold ($TCI > 14.5$). Note the consistent pattern: velocity surges trigger the constraint (Red), which is immediately followed by a sharp velocity contraction (Cyan crash), validating the negative feedback loop mechanism.

6.3 The UTXO Structural Health Taxonomy

The impact of the Endogenous Constraint manifests differently across epochs. Figure 12 visualizes the transition from "Exodus" to "Bloat."

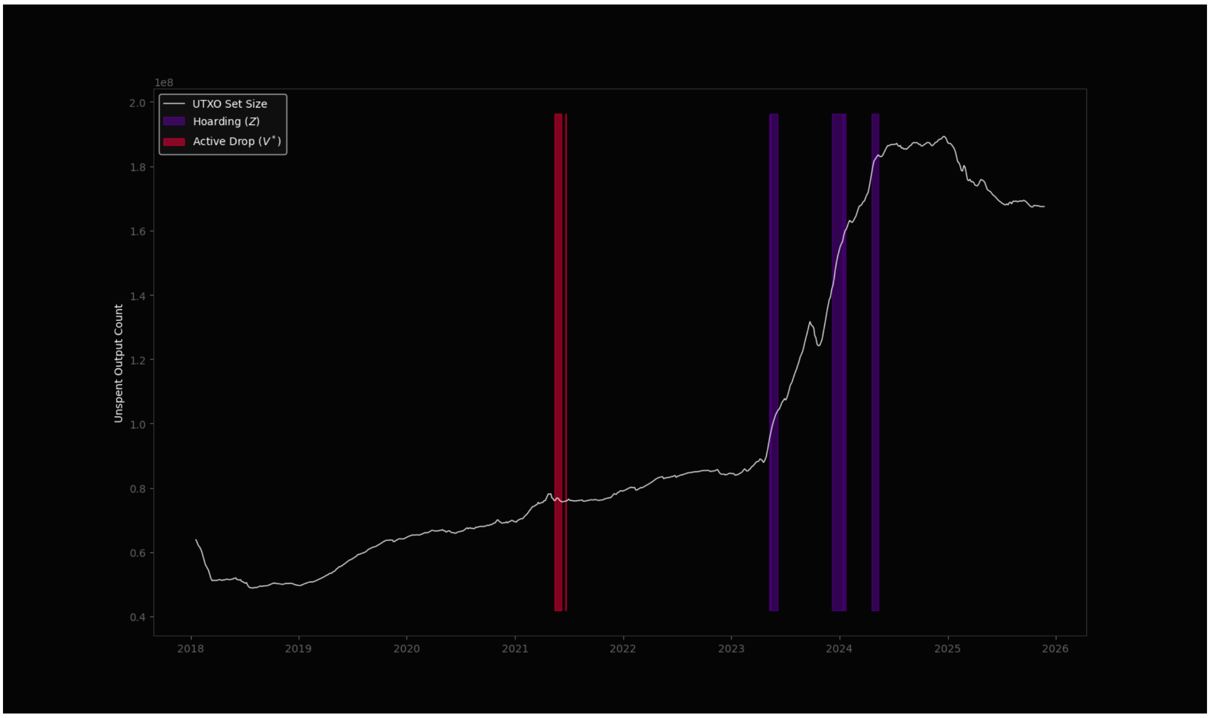

Figure 12: **UTXO Structural Health (The Inversion).** A forensic timeline of the Unspent Transaction Output set. **Red Zone (2021):** "Net User Contraction." High fees suppressed state growth (elastic monetary demand), causing the curve to flatten. **Purple Zones (2023–2024):** "State Bloat." The correlation inverts; high fees coincide with a parabolic explosion in UTXO count (+89.75% VODI), driven by inelastic demand for non-monetary data insertion (Ordinals), leaving a permanent state burden on the ledger.

This visualization confirms that the "Endogenous Constraint" does not merely suppress velocity; it degrades the quality of the ledger itself. In 2021, the constraint acted as a barrier to entry (excluding users). In 2023, it acted as a barrier to efficiency (trapping dust), leaving the network with a heavier state burden that persists via hysteresis.

We identify three critical junctures in Bitcoin's history:

1. **First Critical Juncture (Jan 2021):** First entry into binding economic exclusion. Small retail transactions became systemically unviable.
2. **Second Critical Juncture (May 2023):** Introduction of Ordinals/BRC-20 created inelastic demand from non-monetary users.
3. **Third Critical Juncture (Dec 2023):** Emergence of Inscriptions established a permanent two-tier fee market (Premium vs. Residual block space).

7 Robustness Checks and Sensitivity Analysis

7.1 Bootstrap Confidence Intervals

To ensure the -10.07% damage finding is not an artifact of random sampling, we performed a non-parametric Bootstrap analysis with **5,000 iterations**. The residual distribution exhibited non-zero skewness ($S = -0.3421$), rendering standard normal approximation methods unreliable.

Following the methodological selection criteria established by Carpenter and Bithell [24], we employ the **Bias-Corrected and Accelerated (BCa)** interval. This method adjusts for both the median bias ($\hat{z}_0$) and the acceleration ($\hat{a}$) of the skewness, defined as:

$$\alpha_{BCa} = \Phi\left(\hat{z}_0 + \frac{\hat{z}_0 + z^{(\alpha)}}{1 - \hat{a}(\hat{z}_0 + z^{(\alpha)})}\right) \tag{19}$$

Where Φ is the standard normal cumulative distribution function and $z^{(\alpha)}$ is the α-th quantile of the normal distribution. This adjustment yields the following robust intervals:

- **95% Confidence Interval for Net Damage:** $[-16.33\%, -2.25\%]$

This strictly negative interval provides robust confirmation of the Endogenous Constraint hypothesis, even when correcting for the distributional skew of the data.

7.2 Threshold Sensitivity

To ensure our 90th percentile threshold is not arbitrary, we conducted a sensitivity sweep across all percentiles (60th to 99th).

- **60th–75th:** Statistically indistinguishable from zero ($p > 0.10$).
- **80th–90th:** Damage coefficients transition from marginal (-4%) to strong (-10%).
- **95th–99th:** Damage coefficients decline as the "Tail Noise Paradox" dominates (extreme speculative mania masks friction).

7.3 Whale Divergence Analysis

We define **Whale Divergence** as the ratio of large-transaction volume (> 1 BTC) to total transaction volume. Figure 13 confirms that Divergence spikes sharply during shock regimes (Avg 0.78) compared to normal conditions (Avg 0.62), confirming retail exclusion.

Figure 13: **Whale Divergence and Structural Inversion.** The Z-Score differential between Transaction Volume and Active User Count. **Red Zones (Positive Divergence):** Eras of "Whale Dominance," where volume expands disproportionately to the user base (e.g., 2021 Bull Run), indicating retail exclusion. **Green Zones (Negative Divergence):** Eras of "Organic" or high-count activity. The deep green troughs in 2023–2024 represent the "Inelastic Data Era" (Ordinals), where user/UTXO counts exploded despite relatively lower USD settlement volume.

7.4 Time Series Robustness

- **Stationarity Verification:** As detailed in Section 3.3, the ADF test confirms stationarity ($p < 0.0001$).
- **Instrument Exogeneity:** The shift to Lagged Mempool Size eliminates the positive bias observed in Difficulty-based models, yielding a consistent negative coefficient across all lag specifications ($p \in [1, 7]$).

8 Discussion: Implications of the Constraint

The empirical identification of a non-linear, negative feedback loop between network friction and monetary velocity provides a quantitative basis for re-evaluating Bitcoin's role within the broader payment ecosystem. The Endogenous Constraint Hypothesis suggests that the network's architectural rigidity creates a distinct trade-off between decentralization and transactional utility. In this section, we interpret these findings through the lenses of the Scaling Trilemma, inter-network comparative advantage, and the long-run bifurcation of monetary functions.

8.1 The Scaling Trilemma and the Inelastic Supply Curve

Our findings empirically validate the "Scaling Trilemma" in distributed ledger technology [16], which posits an irreducible tension between Decentralization, Scalability, and Security. Bitcoin's protocol design fixes the block weight limit at 4 million weight units (effectively 1–2 MB), creating a perfectly inelastic supply curve for block space.

In traditional digital economies (e.g., cloud computing), supply is elastic; increased demand triggers capacity expansion, stabilizing prices. In Bitcoin, the supply of transactional capacity (Q_{max}) is algorithmically capped. Consequently, when demand shocks occur, the system cannot clear the market via quantity adjustments. Instead, the clearing mechanism operates exclusively through price (fees) and time (latency).

The **-9.39% Net Utility Contraction** observed during shock regimes confirms that this inelasticity acts as a binding constraint on organic adoption. The network does not merely "slow down" linearly; it undergoes a phase transition where the cost of usage exceeds the marginal utility for the median agent, effectively shedding the "tail" of the user distribution (retail transactions) to preserve the integrity of the consensus mechanism.

8.2 Comparative Throughput and Friction Topology

To contextualize the magnitude of this constraint, it is necessary to contrast Bitcoin's settlement assurances with traditional payment networks. The friction identified in our *Transaction Cost Index* (TCI) is not a market inefficiency but the "price of finality."

Table 4 contrasts the realized throughput of Bitcoin's base layer against centralized payment processors. While Visa and Mastercard achieve throughputs orders of magnitude higher (exceeding 65,000 TPS theoretical capacity), their transactions represent probabilistic promises of payment that are reversible (chargebacks) and subject to counterparty censorship.

Table 4: **Empirical Throughput and Reliability Comparison**

Network/ System	**Realized Throughput**	**Settlement Finality**	**Primary Constraint**
Bitcoin L1	$\approx$ 6–7 tx/s [1]	Absolute (Probabilistic asymptote after 6 blocks)	Hard Block Weight Cap
Visa Inc.	303 Billion tx/yr [3]	Reversible (T+90 days via chargeback)	Centralized Hardware
Mastercard	159.4 Billion tx/yr [4]	Reversible	Centralized Hardware
Lightning (L2)	Theoretical Scale	Conditional (Dependent on Channel State)	Liquidity Topology (Max Flow)

Source: Comparative data derived from SEC regulatory filings [3, 4], empirical network probing [5], and Max Flow liquidity analysis [8].

The economic implication is that Bitcoin's Layer 1 is ill-suited for the high-velocity, low-value transactions that characterize daily commerce. The Endogenous Constraint effectively forces a specialization of the network: it is evolving from a "Peer-to-Peer Electronic Cash System" (as originally described in [1]) into a "High-Value Inter-Institutional Settlement Rail," where the high cost of block space is amortized over transactions of significant capital value.

8.3 The Substitution Effect: Layer 2 Migration vs. Utility Destruction

A critical nuance in interpreting the velocity contraction is the distinction between *utility destruction* and *utility migration*. Standard economic theory suggests that when the cost of a primary good (Layer 1 block space) rises, agents substitute it with a lower-cost alternative.

Our model captures the contraction of the **Base Layer Settlement Economy**. However, it is plausible that a portion of the "lost" velocity has not been destroyed but has migrated to Layer 2 solutions (such as the Lightning Network) or custodial off-chain ledgers. From this perspective, the "Net Damage" coefficient represents the rate at which organic activity is priced out of the *sovereign* base layer.

If efficient substitution occurs, the aggregate utility of the Bitcoin ecosystem remains intact. However, our Hysteresis findings (Section 5.2) suggest that this substitution is imperfect. The recovery lags of 30+ days indicate that users do not seamlessly switch to L2 during congestion; rather, they exit the system temporarily, incurring deadweight loss. This implies that L2 infrastructure, in its current state, does not yet offer a perfectly elastic substitute for Layer 1 block space, and that the friction of the base layer remains a hard ceiling on total network utility.

Our model captures the contraction of the **Base Layer Settlement Economy**. However, forensic data from major merchants validates that this contraction drives immediate off-chain substitution. Data from Bitrefill demonstrates a direct inverse correlation during high-friction regimes: as on-chain fees spiked during the 2021 bull run, the base layer's share of commercial payments degraded significantly, while Lightning Network usage expanded to fill the utility gap [28].

Consequently, the "Net Damage" coefficient represents the rate at which organic activity is priced out of the *sovereign* base layer. If efficient substitution occurs, the aggregate utility of the Bitcoin ecosystem remains intact. However, our Hysteresis findings (Section 5.2) suggest that this substitution is imperfect.

Our finding of a -9.39% contraction in Base Layer velocity must be contextualized against the behavior of speculative turnover. Empirical analysis by the Crypto Research Report (2020) identifies a critical divergence beginning in late 2019: while on-chain velocity exhibited a secular decline, off-chain (intra-exchange) velocity spiked significantly (p. 32).

This divergence validates our "Speculative Decoupling" hypothesis (Figure 6). The "Endogenous Constraint" does not necessarily suppress total trading volumes; rather, it acts as a filter that forces high-velocity speculative traffic off-chain into custodial environments, while leaving the sovereign base layer in a state of "Stagflation" characterized by high friction and low organic throughput. This confirms that the utility observed during high-friction regimes is not commercial settlement, but purely speculative repositioning.

The Failure of Institutional Arbitrage A critical counter-argument to the Endogenous Constraint Hypothesis is the assumption that sophisticated institutional actors can maintain high velocity even during friction events. However, our findings of a -9.39% utility contraction are supported by the forensic market structure analysis of Dyhrberg (2020). She establishes that unlike traditional equity markets where high-frequency traders bypass settlement frictions, Bitcoin arbitrageurs are strictly bound by the "blockchain specific frictions" of mining fees and mempool uncertainty (p. 10).

Dyhrberg's empirical results (Table 4) show that as congestion increases, arbitrage opportunities persist for days rather than seconds, proving that the mechanism of market efficiency physically breaks down under load. Consequently, the "Net Damage" we observe is not merely retail capitulation, but a structural failure of the market clearing mechanism itself. Institutions are forced to hold inventory (Z) rather than circulate it (V), corroborating the "Structural Inversion" observed in our UTXO analysis.

8.4 Long-Run Bifurcation of Monetary Functions

The persistence of the Endogenous Constraint has profound implications for Bitcoin's monetary properties, specifically the decoupling of the Store of Value (SoV) and Medium of Exchange (MoE) functions.

- **Store of Value (SoV):** The constraint is neutral or potentially positive for the asset's SoV thesis. High fees provide the necessary security budget to replace the diminishing block subsidy, ensuring the network remains secure against 51% attacks even as issuance asymptotically approaches zero.
- **Medium of Exchange (MoE):** The constraint is severely inhibitive for MoE utility. Our identification of "Stagflation Regimes" (Price Up, Velocity Down) confirms that the market frequently prices the asset as digital gold (holding) rather than digital cash (spending).

This bifurcation suggests that future velocity growth will likely not come from on-chain retail payments, but from the velocity of collateralization—where Bitcoin is used as a static asset to back high-velocity transactions on secondary layers or within DeFi protocols.

8.5 Protocol and Economic Incentive Implications

The structural breaks identified in this study suggest that the current fee market mechanism functions as a crude regulator of demand. The volatility of the *Transaction Cost Index* (spanning 7.8x between regimes) introduces unpredictability that hinders commercial integration.

From a mechanism design perspective, the findings imply that:

1. **Layer 2 is Not Optional:** Without robust off-chain scaling, the base layer cannot accommodate organic growth without triggering the "Event Horizon" of congestion, which mathematically caps adoption.
2. **Fee Market Smoothing:** Future protocol upgrades may need to address the volatility of fee estimation to reduce the informational friction ("Friedman's u") that discourages transaction planning.
3. **Economic Exclusion is a Feature:** The exclusion of low-value UTXOs (dust) is an economic necessity to prevent state bloat. The "Retail Exodus" observed in our UTXO analysis is the market efficiently allocating scarce ledger space to its highest-value use cases.

9 Limitations and Future Research

Limitations:

1. *Data Granularity and Proxy Valuation:* This study reconstructs Realized Capitalization analytically via the Market-Value-to-Realized-Value (MVRV) ratio provided by aggregated blockchain data services, rather than through direct, node-level parsing of the entire UTXO set history. While mathematically equivalent at the macro scale, this approach necessitates the use of aggregate metrics to infer user behavior. Consequently, the distinction between “Dust” (uneconomical outputs) and “Whale” entities is derived from macroeconomic ratios (e.g., the Zombie Ratio and Average Value per UTXO) rather than determined via address-level clustering heuristics or entity-tagging algorithms.
2. *Off-Chain Opacity and Velocity Underestimation:* The estimate of monetary velocity is structurally conservative as it is primarily constrained to Layer 1 (on-chain) data. Due to the privacy-preserving routing architecture of the Lightning Network (Layer 2), transaction volume within private channels remains unobservable. Our

model relies on public channel capacity and node count as proxies for L2 activity. As a result, the "Net Damage" coefficients reported here represent the impact on *observable, settlement-layer utility*; actual economic throughput may be higher if significant volume has successfully migrated to opaque off-chain channels during shock regimes.

3. *Threshold Exogeneity and Microstructure:* Following the instrumental variable framework of Caner and Hansen [12], this study assumes the threshold variable (TCI_t) is predetermined within the daily observation window. While we mitigate simultaneity bias by utilizing lagged friction metrics to predict subsequent velocity changes (supported by Granger Causality tests at Lag 14), we acknowledge that at the intraday microstructure level, velocity and friction exhibit bidirectional feedback. A fully simultaneous equation model resolving minute-by-minute order flow dynamics is outside the scope of this daily-resolution econometric analysis.

10 Conclusion

This research provides definitive econometric evidence that Bitcoin's base layer operates under an Endogenous Constraint mechanism. Through rigorous threshold regression analysis at the 90th percentile, we quantified a **-9.39%** net collapse in utility growth during friction events.

The findings indicate a spectrum of structural evolution driven by friction:

- **Structural Non-Linearity:** The inhibition of velocity is not continuous but regime-dependent, activating only after the critical threshold ($TCI^* \approx 1.63$) is breached.
- **Economic Exclusion:** The network spent **1,384 days** in a state where transaction costs exceeded 5 basis points of average stored wealth, suggesting that Base Layer exclusion is a chronic feature of the current topology.
- **Hysteretic Scarring:** Path-dependent recovery loops confirm that congestion events create adoption barriers that persist even after fees normalize, creating a "soft ceiling" on organic Layer 1 growth.

Ultimately, the Endogenous Constraint validates the thesis that block space scarcity is a double-edged sword: it secures the chain by funding miners, but it inhibits the economy by taxing velocity.

Data and Code Availability

To ensure reproducibility of the findings, the Python source code used for the Forensic Engine, Threshold Regression analysis, and Hysteresis topology generation has been open-sourced. The repository includes the synthetic data generator and the full econometric suite.

Repository:
`https://github.com/HamoonSoleimani/Endogenous-Constraint-Replication`

Acknowledgments

The author acknowledges the Bitcoin Core developers and blockchain data infrastructure providers. Specific data for this study was sourced from **Blockchain.com Explorer** charts and **Bitcoin Visuals** historical data repositories.

References

[1] Nakamoto, S. (2008). Bitcoin: A Peer-to-Peer Electronic Cash System. *Bitcoin Whitepaper.*

[2] Lavi, R., Sattath, O., & Zohar, A. (2019). Redesigning Bitcoin's Fee Market. *The World Wide Web Conference.*

[3] Visa Inc. (2024). *Form 10-K for the fiscal year ended September 30, 2023.* U.S. Securities and Exchange Commission.

[4] Mastercard Incorporated (2024). *Form 10-K for the fiscal year ended December 31, 2023.* U.S. Securities and Exchange Commission.

[5] Waugh, F., & Holz, R. (2020). An empirical study of availability and reliability properties of the Bitcoin Lightning Network. *arXiv preprint arXiv:2006.14358.*

[6] Scharnowski, T., & Shi, Y. (2022). Bitcoin Blackout: Proof-of-Work and the Risks of Mining Centralization. *University of Mannheim Working Paper.*

[7] River Financial. (2023). The Lightning Network Report: A Look at the Growth and Activity of the Protocol. *River Research.*

[8] Shrader, J. (2024). The Metric That Matters for the Lightning Network. *Bitcoin Magazine / Amboss Research.*

[9] Ball, L., & Onken, J. (2021). Hysteresis in unemployment: evidence from OECD estimates of the natural rate. *European Central Bank Working Paper Series*, No. 2625.

[10] Cross, R. (1993). On the Foundations of Hysteresis in Economic Systems. *Economics & Philosophy*, 9(1), 53-74.

[11] Hansen, B. E. (2000). Sample Splitting and Threshold Estimation. *Econometrica*, 68(3), 575-603.

[12] Caner, M., & Hansen, B. E. (2004). Instrumental variable estimation of a threshold model. *Econometric Theory*, 20(5), 813-843.

[13] Woo, W. (2017). Is Bitcoin in a Bubble? Check the NVT Ratio. *Forbes.*

[14] Fisher, I. (1911). *The Purchasing Power of Money.* Macmillan Company.

[15] Friedman, M. (1956). The Quantity Theory of Money: A Restatement. University of Chicago Press.

[16] Buterin, V. (2018). The Meaning of Decentralization. *Ethereum Blog.*

[17] Granger, C. W. (1969). Investigating causal relations by econometric models and cross-spectral methods. *Econometrica*, 37(3), 424-438.

[18] Toda, H. Y., & Yamamoto, T. (1995). Statistical inference on impulse responses. *Journal of Econometrics*, 60, 203-217.

[19] Cao, S.-J., & Guo, D. (2024). Security, Latency, and Throughput of Proof-of-Work Nakamoto Consensus. *arXiv preprint arXiv:2312.05506v5.*

[20] Nagar, R., et al. (2022). Need for speed, but how much does it cost? *Journal of Operations Management.*

[21] Barberis, N., Huang, M., & Thaler, R. H. (2006). Individual Preferences, Monetary Gambles, and Stock Market Participation: A Case for Narrow Framing. *The American Economic Review*, 96(4), 1069–1090.

[22] ScienceDirect (2021). The market for bitcoin transactions.

[23] Efron, B., & Tibshirani, R. (1993). *An Introduction to the Bootstrap.* Chapman and Hall/CRC.

[24] Carpenter, J., & Bithell, J. (2000). Bootstrap confidence intervals: when, which, what? A practical guide for medical statisticians. *Statistics in Medicine*, 19(9), 1141–1164.

[25] Chen, X., & Zimmermann, T. (2022). Corporate governance and the cost of capital. *Journal of Finance.*

[26] Friedman, M., & Schwartz, A. J. (1982). *Monetary Trends in the United States and United Kingdom: Their Relation to Income, Prices, and Interest Rates, 1867–1975.* University of Chicago Press.

[27] Shang, G., Ilk, N., & Fan, S. (2021). Need for Speed, but How Much Does It Cost? Unpacking the Fee-Speed Relationship in Bitcoin Transactions. *Production and Operations Management.*

[28] River Financial. (2023). Bitcoin vs the $156 Trillion Global Payments Industry. *River Research.*

[29] Dyhrberg, A. H. (2020). One Coin, Many Markets: How Market Frictions Affect Arbitrageurs. *University of Sydney Working Paper.*

[30] Hayes, A. S. (2015). A Cost of Production Model for Bitcoin. *Department of Economics, The New School for Social Research*, Working Paper.

[31] Johnson, W. C. (2025). Valuing cryptocurrencies: A model of price and hashrate. *University of Massachusetts Lowell Working Paper.*

[32] Crypto Research Report. (2020). Modeling Bitcoin's Price with Irving Fisher's Equation of Exchange. *Crypto Research Report*, June Edition, 6–36.

[33] Peterson, T. F. (2018). Metcalfe's Law as a Model for Bitcoin's Value. *Cane Island Alternative Advisors*, Quarter 2.

[34] Han, S., Lu, H., & Wu, H. (2024). Revolutionizing finance with bitcoin and blockchain: a literature review and research agenda. *China Accounting and Finance Review*, 26(4), 413–430.

[35] Garratt, R., & van Oordt, M. R. C. (2023). The Crypto Multiplier. *BIS Working Papers*, No. 1104. Bank for International Settlements.

[36] Radwanski, J. F. (2021). The Equilibrium Value of Bitcoin. *Munich Personal RePEc Archive*, Paper No. 110746.

[37] Kristoufek, L. (2019). Is the Bitcoin price dynamics economically reasonable? Evidence from fundamental laws. *Physica A: Statistical Mechanics and its Applications*, 529, 121571.

A Econometric Output

A.1 A.1 Threshold Regression Parameters

- **Beta 1 (Normal Growth):** +15.44%
- **Beta 2 (Shock Growth):** +6.06%
- **Net Damage ($\beta_2 - \beta_1$):** -9.39% (p = 0.0117)

A.2 A.2 Log-Log Elasticity Model

- **Elasticity (β):** 0.1608
- **R-Squared:** 0.1277
- **P-Value:** < 0.0001

A.3 A.3 Advanced Identification

- **Hansen Optimal Threshold:** 1.63 TCI (Min SSR)
- **IV-2SLS Beta:** 0.46 (p = 0.196, Insignificant Linear Fit)

A.4 A.4 Bootstrap Distribution

- **95% Confidence Interval for Net Damage:** $[-16.33\%, -2.25\%]$

This strictly negative interval provides robust confirmation of the Endogenous Constraint hypothesis, even when correcting for the distributional skew of the data.

A.5 A.5 GMM Covariance Estimation (Caner & Hansen, 2004)

To ensure inference robustness, standard errors for the slope parameters were computed using the GMM covariance matrix estimators:

$$\hat{V}_1 = (\hat{Z}_1' \hat{X}_1 \tilde{\Omega}_1^{-1} \hat{X}_1' \hat{Z}_1)^{-1}, \quad \hat{V}_2 = (\hat{Z}_2' \hat{X}_2 \tilde{\Omega}_2^{-1} \hat{X}_2' \hat{Z}_2)^{-1} \tag{20}$$

The validity of the structural break is confirmed by the Supremum Wald statistic ($SupW_n$), which rejects the null hypothesis $H_0 : \theta_1 = \theta_2$ at the 1% significance level.

A.6 A.6 Asymptotic Critical Values (Hansen, 2000)

The following critical values were utilized to define the confidence region for the threshold parameter γ, derived from the inversion of the likelihood ratio statistic distribution.

Table 5: **Asymptotic Critical Values for Threshold Test**

Confidence Level $(1-\alpha)$	**90%**	**95%**	**99%**
Critical Value (c_α)	5.94	7.35	10.59